Homo- and Copolymerization of Ethylene with Highly Active Catalysts Based on $TiCl_4$ and Grignard Compounds

A. MUÑOZ-ESCALONA, H. GARCÍA, and A. ALBORNOZ,
Laboratorio de Polímeros, Centro de Química, Instituto Venezolano de Investigaciones Científicas, (I.V.I.C.) Apartado 21827, Caracas 1020-A, Venezuela

Synopsis

In this paper, the synthesis of different catalytic systems based on the reduction of $TiCl_4$ by Grignard compounds has been systematically studied. The catalysts exhibited the highest activities when used in the copolymerization of ethylene with *n*-hexene. The profile of the kinetic curves also changed when the comonomer was present during polymerization. By thermal analysis and scanning electron microscopy techniques, it could be found that the incorporation of the comonomer to the polymer chain brings about a decrease in the polymer crystallinities and an increase in the porosities of the growing particles. Due to that, the diffusion of the monomer to the catalytic active centers takes place more easily, consequently increasing the polymerization rate. In addition, catalysts control better the morphology (size and shape) of the nascent polymer particles when used for copolymerization.

INTRODUCTION

The significance of magnesium compounds in the synthesis of highly active Ziegler–Natta catalysts for olefins polymerization have been extensively reported, not only in the technical but also in the scientific literature.[1,2] One of the earliest developments was the Solvay and Cia[3] catalysts based on Mg(OH)Cl as active support. Later on, Mitsui[4] and Montecatini[5] reported much improved catalytic systems by using $Mg(OH)_2$ compounds, mechanically activated by intensive ball-milling, followed by reaction with $TiCl_4$. Different $Mg(OR)_3$ compounds were also used by Hoechst[6] for the preparation of highly active catalysts.

Chien et al.[7] combined mechanical and chemical activation of $MgCl_2$ to obtain high mileage catalysts for propylene polymerization. This method consists also of the ball-milling of the $MgCl_2$, but in the presence of Lewis base such as ethyl benzoate, followed by incorporation of *p*-cresol and $AlEt_3$ at mild conditions. After $TiCl_4$ was incorporated to the modified support, the Ti^{4+} is reduced to lower oxidation active states. External Lewis bases can also be added to improve the catalytic performance of the systems.[8] More recently, Howard et al.,[9] working for Shell, developed highly active catalysts for ethylene polymerization by reduction of $TiCl_4$ with Grignard compounds. However, to our knowledge, a lack of information exists in the scientific literature concerning the morphological control of the nascent polymers using this type of catalysts. On the other hand, $MgCl_2$ can also be activated only

Journal of Applied Polymer Science, Vol. 34, 977–988 (1987)
 CCC 0021-8995/87/030977-12$04.00

chemically, by dissolving it in polar solvents, followed by reaction with $TiCl_4$, with or without SiO_2 as a carrier.[10] By using this technique, catalysts having good morphological control of the nascent polymers could be obtained. More information about the activation techniques and the structural and chemical changes undergone by the $MgCl_2$ as support during preparation of the catalysts has been published by Sivaram and Srinivasan.[11]

In general, it can be seen that the main efforts have been directed toward the synthesis of catalytic systems showing very high polymerization activities, together with good control of the average molecular weight by high response to H_2, and also good control of molecular weight distributions, for the production of a broad range of resin types. Less attention has been paid to the morphology of the nascent polymers. The control of the polymer morphology is very important from an industrial viewpoint. Specially, in those technologies based on gas phase polymerization using fluid-bed reactors like Unipol process, the control of the particle size, shape, and porosity of the catalysts is very important to avoid failure and shutdown of the plant. Also, in the so-called slurry polymerization technologies, the control of the polymer morphology is of vital importance in avoiding formation of a great amount of fine polymer particles, which can cause problems in plant operations.

This paper deals with the synthesis of catalysts for homo- and copolymerization of ethylene with *n*-hexene, by reduction of $TiCl_4$ with different Grignard compounds. One of the main objectives was to show not only catalysts with high activities, but also to learn how polymerization kinetics are influenced by the type of catalysts used. It is also very important to see whether or not the presence of comonomer in the copolymerization could influence the activity of the catalyst and the morphology of the resulting polymers.

EXPERIMENTAL

Materials

Polymerization grade ethylene (99.5%) was supplied by Matheson (U.S.A.). $TiCl_4$ (98.5%) supplied by Merck (W. Germany) and Et_3Al from Ethyl Co. (U.S.A.) were purified by vacuum distillation.

Isopropyl chloride was supplied by Flucka A. G. (Switzerland), while *n*-butyl-, hexyl-, octyl-, decyl-, and tetradecyl chlorides were purchased from Aldrich Co. (U.S.A.). Before using the alkyl chlorides, they were purified by vacuum distillation.

The Grignard compounds were synthesized under dry nitrogen, following usual procedures. The alkyl chlorides were added dropwise to predried Mg powder in ether under stirring. After the reaction was completed, the excess of ether was distilled under vacuum.

Catalyst Synthesis

In a 250-mL stirred vessel, a solution of $TiCl_4$ in *n*-heptane was added to the Grignard regent over 40 min from a dropping funnel. A 1 : 1 Mg/Ti ratio was maintained. The reaction was carried out in a dry box to assure anaerobic and anhydrous conditions, avoiding deactivation.

TABLE I
Catalytic Activities Obtained by Reduction of $TiCl_4$ with Grignard Compounds

Catalyst[a] no.	Ti (%)	Al/Ti	Monomer[b]	Max. activity (kg polym/g Ti × h × atm)	Time max. act. (minutes)	ASPR[c] (kg pol/g Ti × h × atr
13-G6B1	13.4	58	E	—	—	3.48
18-G6B1	13.4	86	E–H(1.03*M*)	—	—	6.62
39-G4C7	9.3	86	E	11.0	29	7.08
40-G4C5	13.3	76	E	7.0	60	—
43-G4C4	11.5	98	E	10.2	48	—
45-G4C7	9.3	143	E–H(1.03*M*)	18.0	11	8.83
49-G4C1	13.5	175	E	13.0	120	6.40
56-G4C1	13.5	126	E–H(0.824*M*)	14.0	16	8.31
62-G3D3	5.5	245	E	3.5	70	2.55
63-G3D3	5.5	250	E–H(0.824*M*)	12.0	15	6.92
64-G3D6	3.4	436	E	—	—	6.19
71-G3D6	3.4	365	E–H(0.824*M*)	21.0	10	8.68
65-G3D4	4.4	263	E	4.1	20	3.09
66-G3D4	4.4	230	E–H(0.824*M*)	21.0	8	9.35
76-G3D4	4.4	225	E–H(1.648*M*)	13.0	20	6.63
68-G3D8	5.7	290	E	—	—	2.27
70-G3D8	5.7	280	E–H(0.824*M*)	—	—	2.30
73-G14A1A	10.2	87	E	3.4	60	2.49
79-G14A1A	10.2	120	E–H(0.412*M*)	15.9	5	—
77-G14A1A	10.2	105	E–H(0.824*M*)	11.8	5	3.65
80-G14A1A	10.2	113	E–H(1.236*M*)	18.0	3	—
81-G14A1A	10.2	180	E–H(1.648*M*)	20.0	4	—
74-G14A1A	13.1	51	E	—	—	1.34
75-G14A1A	13.1	80	E–H(0.824*M*)	—	—	3.40

[a] For catalyst nomenclature see Experimental.
[b] E = ethylene; H = hexene.
[c] Average specific polymerization rate (see polymerization procedure).

The total amount of Ti in the catalysts was determined as its peroxide by calorimetric methods using a UV Unicam SP 1800 spectrometer.

The catalysts are labeled with numbers and letters (e.g., Table I). The first number before the hyphen corresponds to the run number of the polymerization experiments. The capital letter G followed by a number (i.e., G6) means the number of carbon atoms of the Grignard compound used for catalyst synthesis (e.g., G6 identified the Mg hexyl chloride, G3 the Mg isopropyl chloride, and so on). The last letter followed by a number identifies the batch for catalyst preparation (e.g. B1, C7, A1A, etc.)

Polymerization Procedures

Details on the polymerization procedures have been described elsewhere.[12] Polymerizations were carried out in a batch 0.5-L stirred glass autoclave supplied by Büchi (Switzerland), at 50°C under constant monomer pressure, 1200 rpm, and *n*-heptane as reaction medium. The solid catalysts, sealed in glass ampules, were introduced in the reactor containing 350 mL of *n*-heptane. Then, the reactor was pressurized at 5 atm with ethylene, followed by the addition of 1 mL of the alkyl aluminum as cocatalyst. The polymerization was timed just after breaking the ampules containing the catalysts. The polymeri-

zation rates were determined from the rates of monomer consumption, measured as volumes of ethylene flow into the reactor using a two-buret system similar to that described by Schnecko et al.[13]

After the polymerization was finished, a solution of ethanol containing hydrochloric acid was injected into the reactor and the polymerization quenched. The polymers were washed several times with water-diluted ethanol and dried under vacuum at 50°C. The average specific polymerization rate (ASPR) was calculated over the whole polymerization time and expressed as g polym/g Ti × h × atm. In case of the ethylene copolymerization, a certain amount of *n*-hexene (0.824*M*, except where otherwise noted) was added to the *n*-heptane, and the experiment carried out as previously described for the homopolymerization of ethylene.

Polymer Characterization

The produced polyethylenes were characterized by their intrinsic viscosities, densities, melting points, crystallinities, and nascent morphologies. Viscosimetries were performed in Ubbelohde suspended level viscosimeter. The intrinsic viscosities of the samples were determinated at 135 ± 0.05°C in decalin as solvent. From viscosities average molecular weights were calculated using the relationship[12]

$$[\eta] = 6.2 \times 10^{-4} \times \overline{M}_v^{0.70} \text{ (dL/g)}$$

Polymer densities were measured on molded samples employing density gradient column techniques. The density gradient was prepared according to ASTM D1505-68 method.[14] The flotation solvents used to prepare the density gradient were a mixture of toluene and CCl_4 covering a density range of 0.8000–0.9799 g/mL. All measurements were carried out at 23°C. The density values were also used to calculate the degree of crystallinity of the samples, assuming a two-phase system for the polymer and that the contributions to the specific volume from the amorphous and crystalline phases are additive. The following relation was used:

$$\text{crystallinity (\%)} = \frac{\rho_c}{\rho} \times \frac{\rho - \rho_a}{\rho_c - \rho_a} \times 100$$

where ρ is the density of the sample and ρ_a and ρ_c are the density of the amorphous and crystalline phases, which are taken as 0.854 g cm^{-3} [3,15] and 1.005 g cm^{-3} [3,16] respectively.

The melting points were determined from the peaks of differential scanning calorimetric (DSC) curves obtained with a DuPont DSC 900. The abscissa was calibrated using high purity standards. Sample weights were about 4–6 mg and the scanning rate was 10°C/min. Two scans were recorded to obtain the melting peak of the nascent polyethylene samples and the melting peak from the recrystallized samples. The two curves were conducted at constant scan rate, forward and reverse. From the heat of fusion values, the crystallinity percentage of the polyethylene samples may also be calculated, utilizing the

relation

$$\text{crystallinity (\%)} = \frac{\Delta H_f}{\Delta H_f^*} \times 100$$

where ΔH_f is the heat of fusion of the sample as determined from the DSC curves, and ΔH_f^* is the thermodynamic heat of fusion folded-chain polyethylene crystals, which is taken as 66 cal g^{-1}.[1,17]

The nascent morphology of the produced polyethylene was examined in a scanning electron microscope using an accelerating voltage of 20 kV. The samples were coated with a layer of gold approximately 20 Å thick by sputtering to increase the surface conductivity, avoiding electrostatic discharges during observations.

RESULTS AND DISCUSSION

Catalyst Activities and Polymerization Behavior

Catalysts are very sensitive to the type and amount of cocatalysts used for activation. Thus, in order to obtain high activities, an unusually high amount of cocatalyst with high alkylating power has to be employed, as is shown in Table II. It can be seen that the best cocatalyst is Et_3Al; when $(iso\text{-}bu)_3Al$ is used, catalytic systems with rather low activities were obtained. Using Et_3Al and high Al/Ti ratios, the catalytic systems were employed for homo- and copolymerization of ethylene. In Table I, the maximum activities and the time for reaching them, are given. The specific average polymerization rates have been also included. It can be observed that the type of Grignard compounds used for catalyst preparation has no influence on the catalytic activity. However, the polymerization activity is greatly influenced by the presence of the comonomer *n*-hexene. Thus, in the case of the G3D3 catalyst, a maximum activity of 3.5 kg PE/g Ti × h × atm. was obtained for the homopolymerization of ethylene, while in the copolymerization of ethylene with 0.824*M* of *n*-hexene the catalytic activity increases up to 12.0 kg PE/g Ti × h × atm.

TABLE II
Effect of the amount and Type of Cocatalyst Activity of Grignard-Compounds-Reduced $TiCl_4$

Catalyst no.[a]	Cocatalyst[b]	Al/Ti	Polym time (h)	Amount of polymer (g)
G6B1	TEA	58	1.5	158.0
G6B1	TIBA	61	1.5	0.5
G4C7	TEA	86	0.75	108.0
G4C7	TIBA	84	1.5	10.0
G4C1	TEA	175	3	191.0
G4C1	TIBA	170	1	7.0
G4C5	TEA	76	1.5	155
G4C5	TIBA	110	0.3	0
G4C3	TEA	91	2.6	162.0
G4C3	TIBA	66	1.5	1.0

[a] For catalyst nomenclature, see Experimental.
[b] TEA = Et_3Al; TIBA = $(iso\text{-}bu)_3Al$

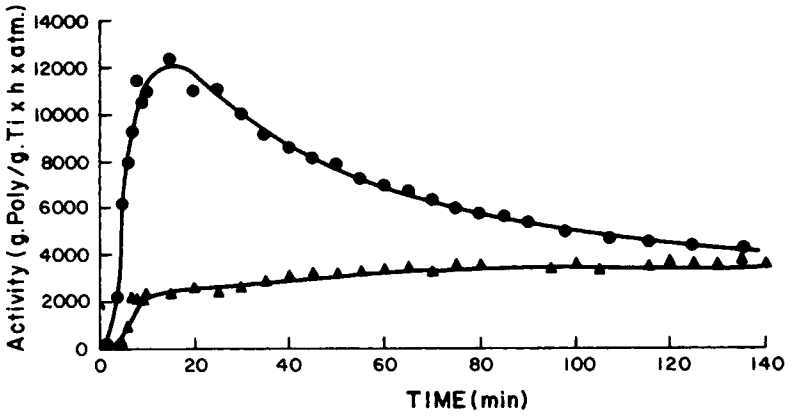

Fig. 1. Profile of kinetic curves for the homopolymerization of ethylene with catalyst 62-G3D3 (▲) and for copolymerization of ethylene with 0.824*M* of *n*-hexene using the same catalyst 63-G3D3 (●) (see Table II). Cocatalyst $AlEt_3$, 50°C, and 5 atm.

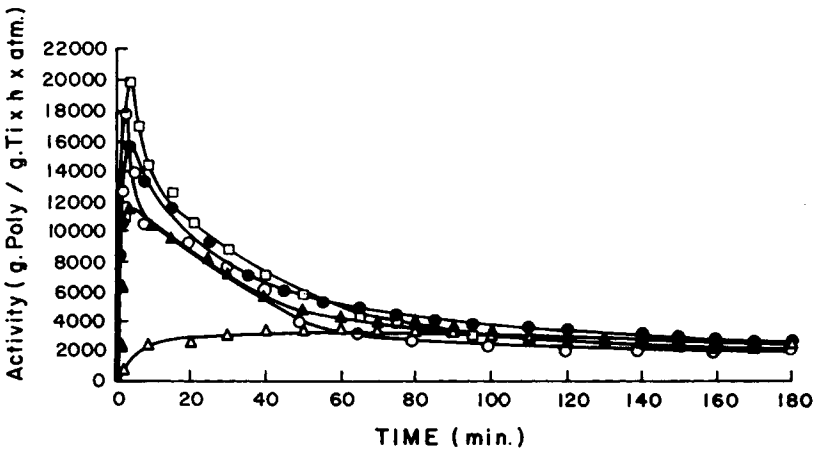

Fig. 2. Profile of kinetic curves for homopolymerizations of ethylene with catalysts G-14A1A (△) and copolymerization with different amount of *n*-hexene: (▲) 0.824*M* (77-G14A1A); (●) 0.412*M* (79-G14A1A); (○) 1.236*M* (80-G14A1A); (□) 1.648*M* (81-G14A1A). Cocatalyst $AlEt_3$, 50°C, and 5 atm.

Furthermore, all catalysts showed decay type kinetic curves, especially in the case of the copolymerization of ethylene with *n*-hexene. In fact, polymerization took place immediately after the catalyst components were mixed. Consequently, the polymerization rate increased very rapidly until a maximum activity was reached. Afterwards, the polymerization rate starts to decay. In the case of the homopolymerizations, however, the observed catalytic activities were much lower, giving rise to profile kinetic curves of acceleration types. Some time they also show a very short induction period, i.e., the polymerization rate increases first slowly, reaching a steady-state value, which remains unchanged for a long time (see Figs. 1 and 2). In some cases the polymerization rate increases again and then starts to decrease. This peculiar behavior of the kinetic curves might be due to the formation of new active centers as the polymerizations proceeds.

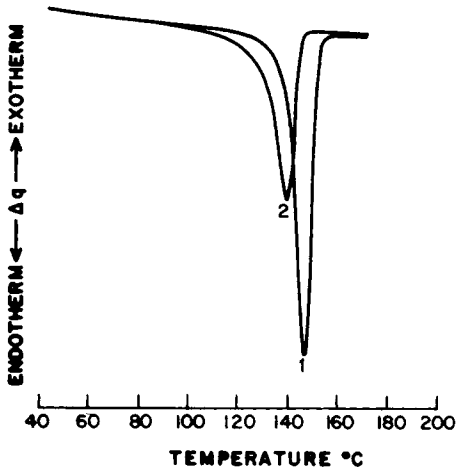

Fig. 3. DSC thermograms of polyethylene homopolymer obtained with catalyst G-14A1A: (1) as produced; (2) after being recrystallized from the melt. Scan rate = 10°C/min.

The increase of the catalytic activity by the presence of the comonomer is far from being understood and is a challenging research goal. To solve this question, a good understanding of the underlying chemical and physical problems is needed. It could be speculated that by reaction of the active centers with the comonomer, new active centers could be formed with more suitable ligand environment, increasing, therefore, the catalytic activity. On the other hand, it could be presumed that the incorporation of the comonomer to the polyethylene chain promotes a decrease in the crystallinity of the polymer layer, covering the catalyst particle, allowing the monomer to diffuse more easily toward the growing polymer particle. In the following, we shall

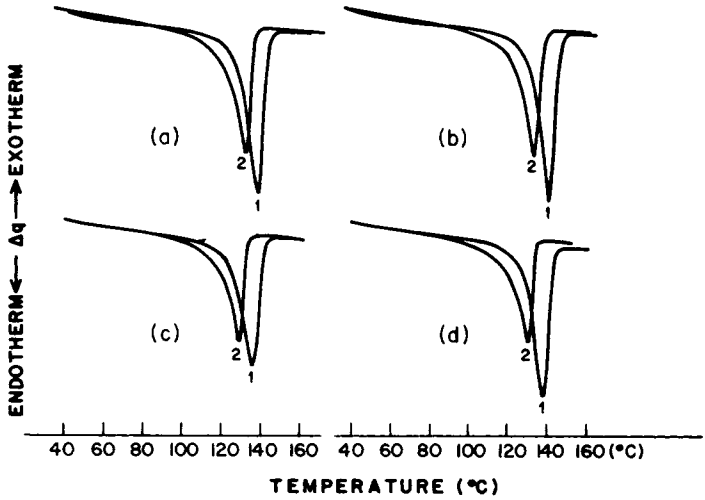

Fig. 4. DSC thermograms of as-produced (1) and recrystallized (2) copolymers of ethylene obtained with catalyst G-14A1A and differents amounts of *n*-hexene: (a) 0.412*M*; (b) 0.824*M*; (c) 1.236*M*; (d) 1.648*M* (see Table II). Scan rate = 10°C/min.

TABLE III
Physicochemical Characteristics of As-Polymerized PE Obtained with Catalysts Based on Grignard-Compounds-Reduced $TiCl_4$

Sample no.	Density (g/mL)	Melting peak (°C)		Crystallinity (%)		
		[a]	[b]	From density	From DSC [c]	From DSC [d]
73-G14A1A	0.9340	144	137	57.0	58	43
77-G14A1A	0.9240	137	130	50.4	40	33
79-G14A1A	0.9240	139	131	50.4	47	38
80-G14A1A	0.9230	133	127	49.7	44	35
81-G14A1A	0.9183	136	128	46.6	42	30

[a] Obtained from as-polymerized samples.
[b] After melting and recrystallization.
[c] From as-polymerized samples.
[d] From remelted samples.

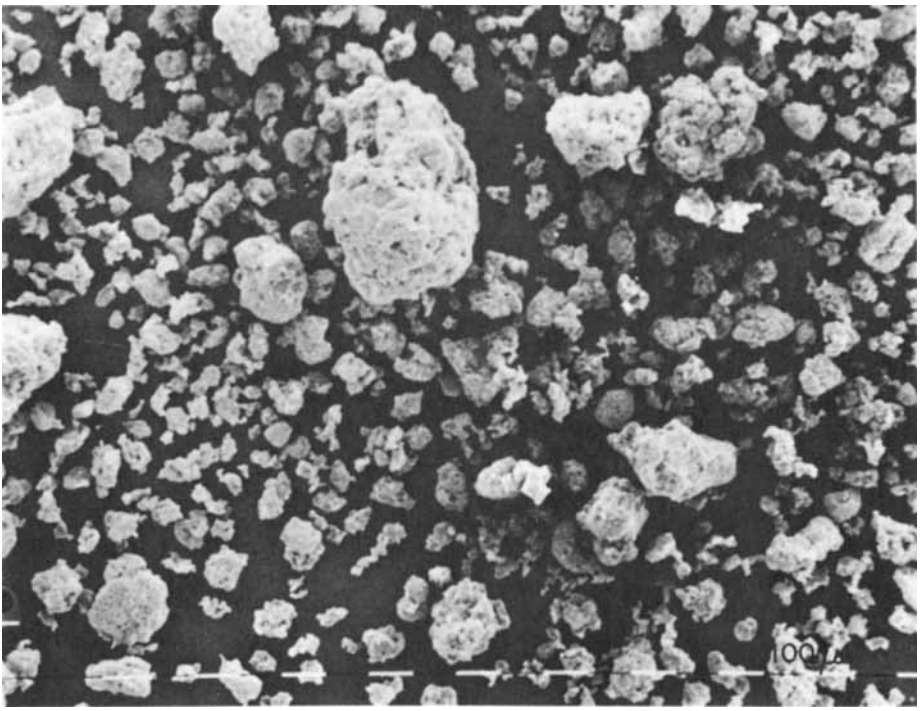

(a)

Fig. 5. SEM micrographs of polyethylene homopolymer obtained with catalyst G-14A1A: (a) general view of polymer particles; (b) at higher magnification.

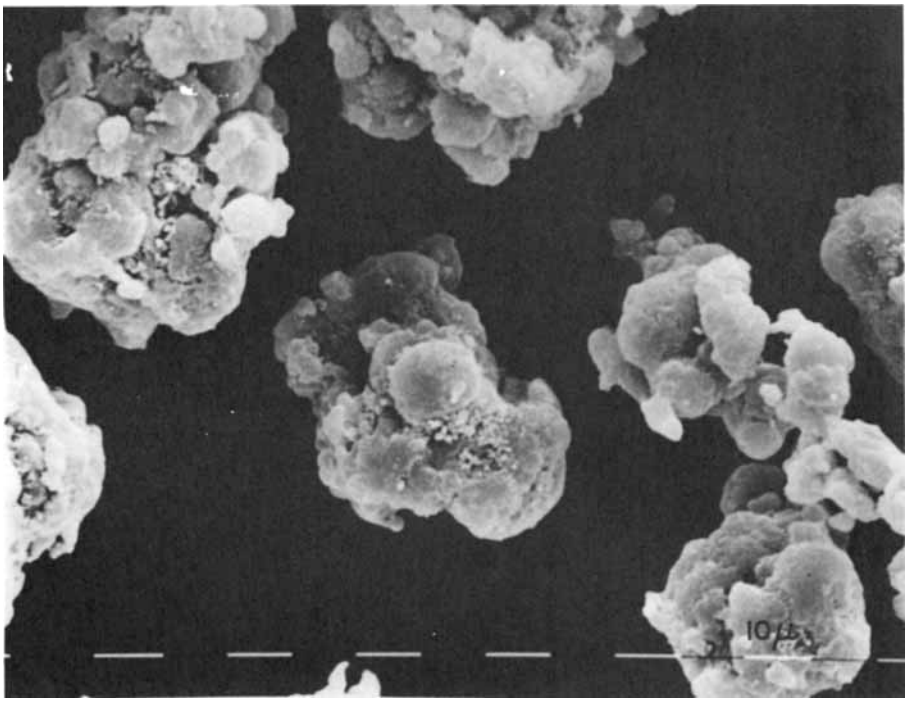

(b)

Fig. 5. (*Continued from the previous page.*)

study the physicochemical characteristics of the nascent polymer in order to answer these questions.

Polymer Characterization

In Figures 3 and 4 the DSC thermograms of the nascent polymer samples (curves 1) and also the second melting curves obtained after being recrystallized from the melts (curves 2) are given. The curves are very informative in their qualitative trends. It can be observed that each one of the as-polymerized homo- or copolymer samples exhibit higher melting temperature and also narrower melting peaks than the recrystallized ones. These results indicate that the nascent polymers have more ordered and regular crystals than those obtained from the melts.

Similar results have been reported in the literature[18,19] in the case of the nascent structure and morphology of polyethylene obtained with $TiCl_3$–AA commercial Ziegler–Natta catalyst. Therefore, the higher structural and morphological order produced in the nascent polyethylene samples might hinder the monomer diffusion toward the catalytically active centers.

On the other hand, in the copolymer of ethylene with *n*-hexene, nascent polymers with lower melting point are produced. This fact indicates higher disordered crystal structure in the copolymers, which favors monomer diffusion in the growing polymer particles. The above results were confirmed by determining the percentage of crystallinity by densities and heat of fusion of

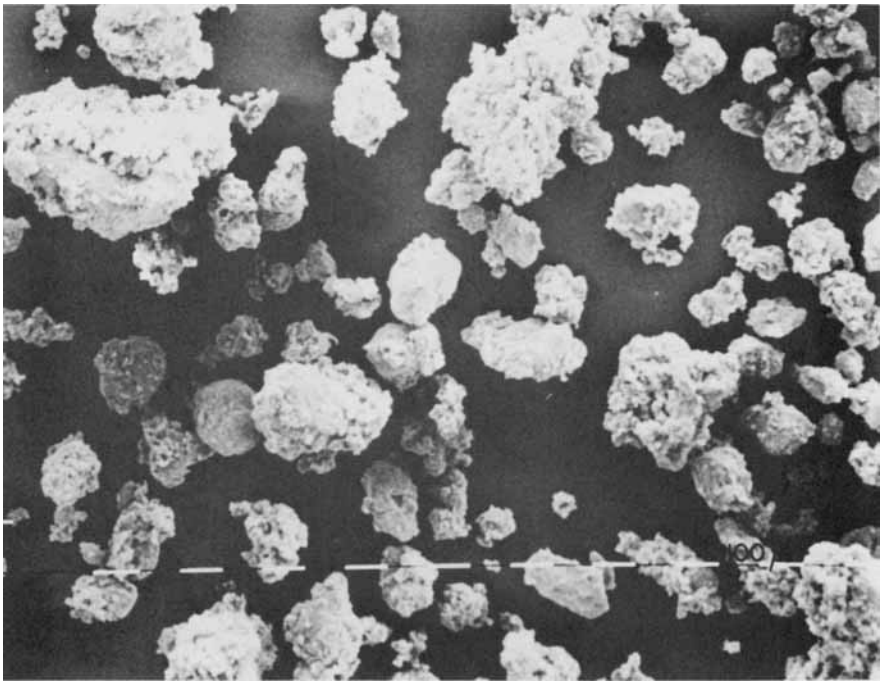

(a)

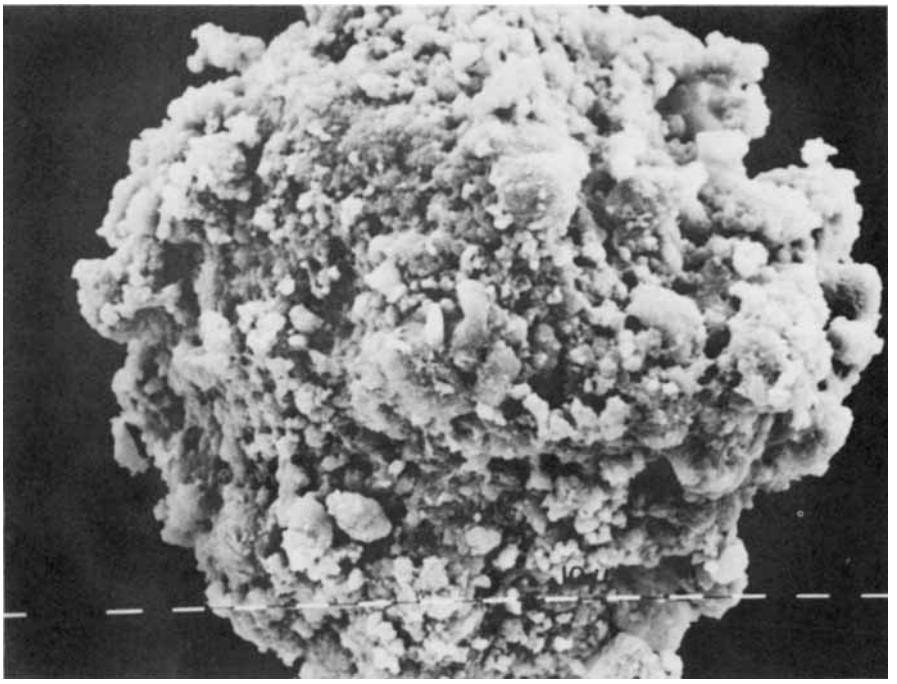

(b)

Fig. 6. SEM micrographs of the copolymer of ethylene with 1.236M of n-hexene (catalyst no. 80-G14A1A, see Table II): (a) general view: (b) details of the particle surface.

the samples (Table III). Although the crystallinity values are in general low, due to very high molecular weights of the polymers ($8–16 \times 10^5$), it is evident that the as-polymerized samples have higher crystallinities than the recrystallized ones. Also, it can be seen that the copolymerization of ethylene with *n*-hexene produce polymers with higher amorphous content and irregular structure that in the homopolymerization of ethylene. This may partially account for higher activities of the catalysts when used for copolymerization. It may be due to the enhancement of the diffusion process during copolymerization.

Morphology of Nascent Polymers

In looking for more evidences supporting the forementioned results, morphologics of the nascent homo- and copolymers were examined using a scanning electron microscope. In addition, the size, shape and porosity of the polymer particles are very important for an industrial viewpoint.

In Figure 5(a), a general view of polyethylene particles obtained by homopolymerization of ethylene is shown. Polyethylene granules, very irregular in shape and size, were produced with all investigated catalytic systems, indicat-

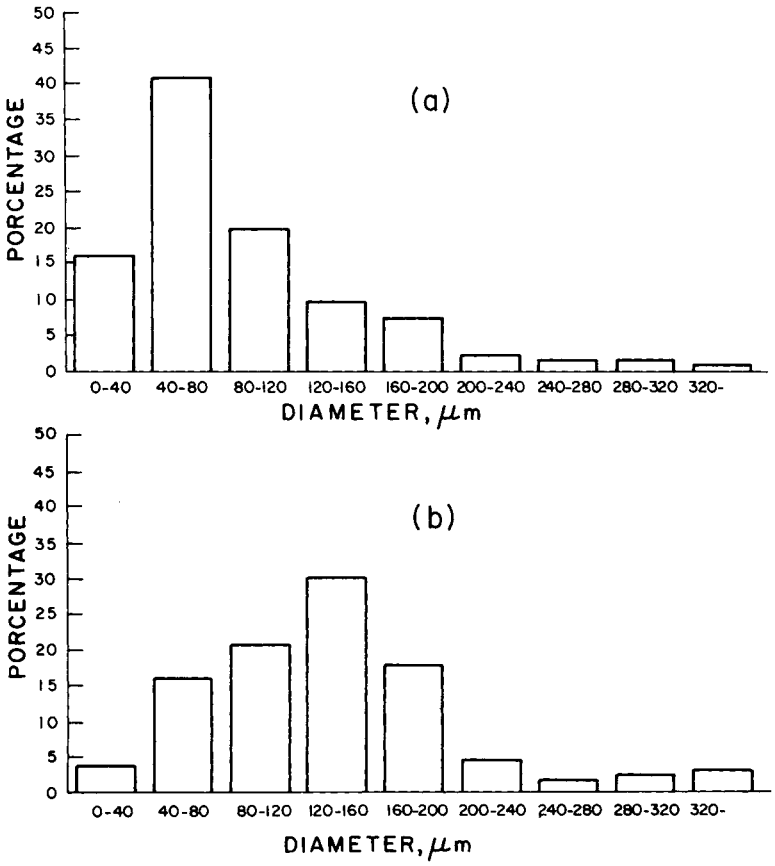

Fig. 7. Polymer particle size distribution of polyethylene homopolymer (a) and copolymer (b) with 1.236*M* of *n*-hexene.

ing that they have poor ability in controlling particle morphology. The structural details of the particles were able to be observed at higher magnification [Fig. 5(b)]. They were formed by agglomerations of very dense subparticles burying deep inside many potentially active centers, which remain blocked to the monomer. On the contrary, when using the catalysts for copolymerization of ethylene with *n*-hexene, better control of the polymer morphology was obtained. Polyethylene granules more uniform in size and more spherical in shape were produced [Fig. 6(a)]. Structural changes were also noted. Thus, very porous particles were, in this case, obtained [Fig. 6(b)]. This allows monomer diffusion, toward the particles, expanding them by the polymer growing inside, and exposing more catalytic centers to the polymerization. As a result, high polymerization activities can be achieved.

Consequently, the polymer particles grow bigger in diameter as can be seen in Figure 7. The average particle size changes from 80 to 160 μm, due to the effect of the *n*-hexene in the polymerization of ethylene.

References

1. Montedison, Belg. Pats. 728,002, 744, 221 (1968).
2. A. Muñoz-Escalona and J. Villalba, *Polymer*, **18**, 179 (1977).
3. Solvay, Belg. Pat. 650.679 (1963).
4. Mitsui Petrochemical, Jpn. Pat. 7,040,295 (1967).
5. Montedison, Belg. Pat. 747,846 (1969).
6. K. Weissermel, H. Cherdron, H. Berthold, B. Diedrich, K. D. Keil, K. Rust, H. Strametz, and T. Toth, *J. Polym. Sci. Symp.*, **51**, 187 (1975).
7. J. C. Chien, J. Wu, and C. I. Kuo, *J. Polym. Sci., Polym. Chem. Ed.*, **20**, 2010, 2445, 2461, (1982).
8. J. C. Chien, J. Wu and C. I. Kuo, *J. Polym. Sci., Polym. Chem. Ed.*, **21**, 725, 737 (1983).
9. R. N. Howard, A. N. Rooper, and K. L. Fletcher, *Polymer*, **14**, 365 (1973).
10. K. Soga, presented at the American Chemical Society in meeting, Miami, FL, April–May 1985.
11. S. Sivaram and P. R. Srinivasan, in *Recent Advances in Polyolefins*, ACS Meeting, Chicago, September 1985.
12. A. Muñoz-Escalona, J. G. Hernández, and J. A. Gallardo, in *Recent Advances in Polyolefins*, ACS Meeting, Chicago, September 1985.
13. H. Schnecko, M. Reinmaller, K. Weirauch, W. Lintz, and W. Kern, *Makromol. Chem.*, **69**, 105 (1963).
14. ASTM D 1505-68, Vol. 27, Am. Soc. for Testing and Mater., Philadelphia, 1972.
15. M. L. Richardson, P. J. Flory, and J. B. Jackson, *Polymer*, **4**, 221 (1963).
16. S. Kavesh and J. S. Schultz, *J. Polym. Sci., A-2*, **8**, 243 (1970).
17. M. Dole, *Forsch. Hochpolym. Forsch.*, **2**, 221 (1960).
18. A. Muñoz-Escalona and A. Parada, *Polymer*, **20**, 274, 859 (1979).
19. A. Muñoz-Escalona and A. Parada, *J. Cryst. Crowth*, **48**, 250 (1980).

Received October 14, 1986
Accepted January 13, 1987